ARMY RESEARCH LABORATORY

Oxygen Diffusion Through Ytterbium-Oxide/ Yttrium-Barium-Cuprate Bilayers

Steven C. Tidrow, Richard T. Lareau, William D. Wilber,
Arthur Tauber, Donald W. Eckart, Robert L. Pfeffer
and Robert D. Finnegan

ARL-TR-940 July 1996

NOTICES

Disclaimers

The findings in this report are not to be construed as an official Department of the Army position, unless so designated by other authorized documents.

The citation of trade names and names of manufacturers in this report is not to be construed as official Government endorsement or approval of commercial products or services referenced herein.

REPORT DOCUMENTATION PAGE

Form Approved
OMB No. 0704-0188

1. AGENCY USE ONLY *(Leave blank)*	2. REPORT DATE	3. REPORT TYPE AND DATES COVERED
	July 1996	Technical Report

4. TITLE AND SUBTITLE

Oxygen Diffusion through Ytterbium-Oxide/Yttrium-Barium-Cuprate Bilayers

5. FUNDING NUMBERS

6. AUTHOR(S)

Steven C. Tidrow, Richard T. Lareau, William P. Wilber, Arthur Tauber,*
Donald W. Eckart, Robert L. Pfeffer, Robert D. Finnegan

7. PERFORMING ORGANIZATION NAME(S) AND ADDRESS(ES)

US Army Research Laboratory (ARL)
Physical Sciences Directorate
ATTN: AMSRL-PS-PC
Fort Monmouth, NJ 07703-5601

8. PERFORMING ORGANIZATION REPORT NUMBER

ARL-TR-940

9. SPONSORING/MONITORING AGENCY NAME(S) AND ADDRESS(ES)

10. SPONSORING/MONITORING AGENCY REPORT NUMBER

11. SUPPLEMENTARY NOTES

Supported in part by the National Research Council.
*Consultant to Geo-Centers Inc., 615 Hope Road, Eatontown, NJ 07703.

12a. DISTRIBUTION/AVAILABILITY STATEMENT

Approved for Public Release: Distribution is Unlimited

12b. DISTRIBUTION CODE

13. ABSTRACT *(Maximum 200 words)*

We have studied the rate of oxygen diffusion through ytterbium oxide, a buffer and dielectric layer used in high critical temperature superconducting (HTSC) structures. An epitaxial bilayer film of ytterbium oxide on yttrium-barium-cuprate (YBCO) was deposited onto an (001) oriented single crystal MgO substrate using the pulsed laser deposition technique. The rate of oxygen diffusion through the bilayer was investigated from 365 to 655 °C by post deposition annealing individual sections of the bilayer in 0.5 atm of oxygen-18 enriched molecular oxygen gas. Secondary ion mass spectroscopy was used in depth profile oxygen-18 and oxygen-16 in each sample. Oxygen diffusion coefficients for ytterbium oxide at 365, 465, 555 and 655 °C were determined to be roughly (6, 16, 360 and 200) x 10^{-14} cm^2 s^{-1}, respectively. For temperatures greater than about 500 °C, these diffusion rates can limit oxygen intake into underlying YBCO films; therefore, HTSC multilayer devices that utilize ytterbium oxide as a dielectric layer may require longer annealing cycles in order to fully oxygenate each underlying HTSC layer.

14. SUBJECT TERMS	15. NUMBER OF PAGES
High critical temperature superconductors; HTSC; ytterbium oxide; oxygen diffusion; bilayers	15
	16. PRICE CODE

17. SECURITY CLASSIFICATION OF REPORT	18. SECURITY CLASSIFICATION OF THIS PAGE	19. SECURITY CLASSIFICATION OF ABSTRACT	20. LIMITATION OF ABSTRACT
Unclassified	Unclassified	Unclassified	UL

CONTENTS

LIST OF FIGURES

LIST OF TABLES

OXYGEN DIFFUSION THROUGH YTTERBIUM-OXIDE/YTTRIUM-BARIUM-CUPRATE BILAYERS

INTRODUCTION

Since the discovery of high critical temperature superconductors (HTSCs) [1], there has been a search for appropriate materials on which to grow epitaxial films for device applications. The ideal material is chemically compatible and has both a good structural and thermal expansion match to the HTSC [2,3]. For microwave devices [2-7], the material should also have either a relatively high or low dielectric constant and be low loss and isotropic with respect to microwave radiation. High dielectric constants are needed for delay lines; while low dielectric constants are needed for numerous other microwave devices.

Because of their relatively low dielectric constant and isotropic properties, C sesquioxides are being investigated [8-10] for use as substrates and buffer/dielectric layers in HTSC microwave devices. Ytterbium oxide (Yb_2O_3) has a dielectric constant near 11 and loss tangent ($\tan \delta$) $\cong$ 10^{-2} at 10 kHz, 297 K [11]. Yb_2O_3 is cubic with a lattice constant of 10.4360 Å and linear thermal expansion coefficient [12] of 5-10 x 10^{-6} K^{-1}. The Yb_2O_3 lattice grows c-axis oriented on c-axis oriented Yttrium-Barium-Cuprate $YBa_2Cu_3O_{7-\delta}$ (YBCO). For such growth, the in-plane relationship is likely <100>Yb_2O_3|| YBCO<110> [8]. In such an arrangement, the Yb_2O_3 lattice matches to a quadrupled *a* and *b* lattice parameter of YBCO within 3.4 and 5.2% where the *a* and *b* lattice parameters of YBCO are in compression.

A concern in YBCO multilayer device processing is oxygen uptake in YBCO layers that lie underneath dielectric layers. At the deposition conditions for growth of YBCO [13], the films are oxygen deficient. Providing enough oxygen to thin single layer YBCO films in short annealing cycles, typically 10 to 20 min, has not been difficult due both to the fast oxygen diffusion rates along the *a* and *b* crystallographic axes (> 10^{-13} cm^2 s^{-1} above 300 °C) and the defect nature of the material which provides short circuit diffusion paths along the slow diffusing *c* axis direction ($\cong$ 10^{-16} cm^2 s^{-1} at 400 °C) [14-17]. However, when a dielectric layer is deposited over an oxygen deficient YBCO film, fully oxygenating the YBCO film during reasonably short annealing cycles may prove impossible. Oxygen intake into the YBCO film is impeded whenever the dielectric layer is a good quality, pinhole-free film that diffuses oxygen more slowly than YBCO. Ultimately, oxygen diffusion rates through materials used in HTSC multilayer structures must be determined in order to know the annealing time required to fully oxygenate HTSC layers in the structure.

Here, we report the diffusion rate of oxygen through an epitaxial Yb_2O_3/YBCO bilayer grown on an (001) oriented MgO single crystal substrate. The bilayer was prepared using the pulsed laser deposition (PLD) technique [18,19]. An MgO 1 cm x 1 cm substrate was pasted onto an inconel block with silver paint. The YBCO layer was deposited in 150 mTorr of oxygen and at a block temperature of 850 °C (substrate surface temperature of 815 °C as measured using a 2-14 μm infrared pyrometer with emissivity ε=0.86) by irradiating a YBCO target for 10 min at a laser fluence of 1-2 J/cm^2 using a KrF excimer laser (λ=248 nm) operating at 10 Hz. The Yb_2O_3 layer was deposited at 850 °C in 150 mTorr oxygen using a laser fluence of 1-2 J/cm^2 and a repetition rate of 30 Hz for 15 min. The bilayer film was cooled in 0.5 atm of oxygen from a block temperature of 650 to 450 °C in 15 min and to room temperature over the next 5 min.

The crystallinity and orientation of the bilayer were evaluated with x-ray diffraction θ–2θ scans using copper Kα as the radiation source. The x-ray spectrum of the Yb_2O_3/YBCO bilayer on (001) MgO is shown in Fig. 1. The diffraction peaks indicate an oriented (00ℓ) Yb_2O_3 layer on an oriented (00ℓ) YBCO layer. Using an a.c. eddy current technique [20], the as-grown bilayer was measured to have a critical transition temperature (T_c) onset of 79 K and critical transition temperature ΔT_c of 10 K with two distinct transitions, 2 and 8 K wide, respectively. The film thicknesses of the bilayer were measured to be 16,000/8000 Å for Yb_2O_3/YBCO using scanning electron microscopy (SEM). Rutherford Backscattering Spectroscopy (RBS) revealed film thicknesses of 7100/7100 x 10^{15} atoms/cm^2, respectively. The films were determined to be about 65/100% dense by comparing the RBS and SEM results. Theoretical crystal densities of 7.05/7.50 x 10^{22} atoms/cm^3 were used to convert the RBS values to thickness.

The bilayer was cut into four smaller pieces. Using the annealing procedure described elsewhere [21], each singular piece was annealed in a quartz tube for either 3, 5, 9 or 12 min at 655, 555, 465 and 365 °C, respectively, in 0.5 atm of oxygen consisting of equal parts of oxygen with mass-18 (^{18}O) and oxygen with mass-16 (^{16}O). The tube was then quenched in a cold water bath to less than 100 °C in about 2.5 min. The annealing and quenching technique assures that the majority of diffusion occurs at the given annealing temperature. The bilayers were analyzed for ^{18}O and ^{16}O concentrations as a function of depth using a Cameca IMS-3f secondary ion mass spectrometer (SIMS). A cesium ion (Cs^+) primary ion beam with an impact energy of 14.5 keV was used to sputter the sample. The beam was rastered over a 125 μm x 125 μm area; sputtered ions were collected from a circular region 35 μm in diameter to eliminate crater and edge effects. Negative secondary ions were detected to maximize the oxygen signal.

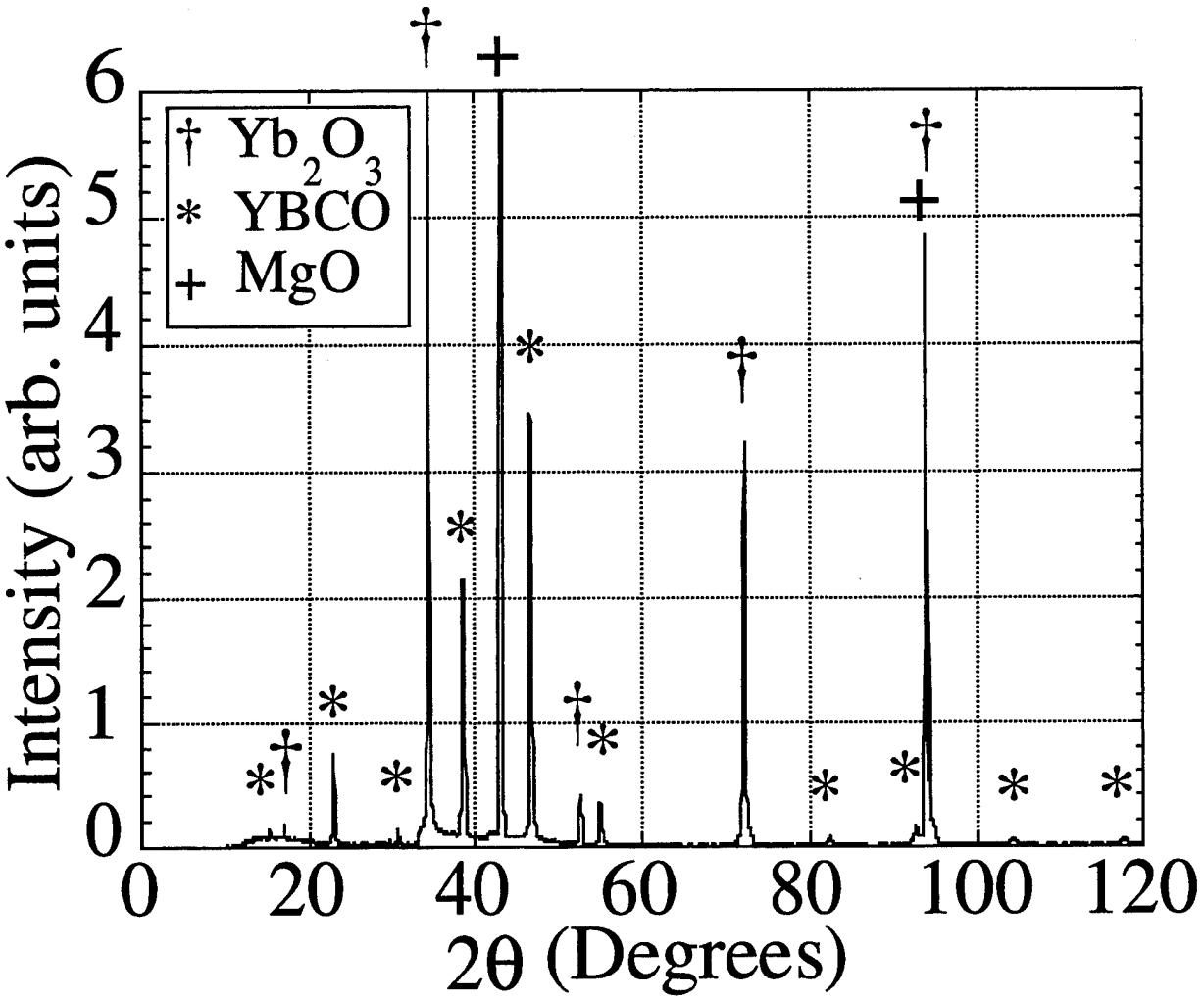

FIGURE 1. X-ray diffraction data, θ–2θ scans, from the Yb_2O_3/YBCO bilayer on (001) MgO substrate. The (00ℓ) diffraction peaks from the MgO substrate, YBCO and Yb_2O_3 layers which are marked "+","*" and "†", respectively, indicate c-axis orientation.

For a sample annealed in a gas mixture of oxygen containing equal parts of ^{18}O and ^{16}O, the concentration of diffused oxygen in the bilayer at depth x, $C_D(x)$, can be expressed as:

$$C_D(x) \equiv \frac{2[(^{18}O) - 0.00204(^{18}O + ^{16}O)]}{[(^{18}O + ^{16}O)]} \qquad (1)$$

where (^{18}O) and (^{16}O) represent the number of SIMS counts of ^{18}O and ^{16}O isotopes at depth x, respectively. The term $0.00204(^{18}O + ^{16}O)$ represents the natural abundance level or background level of ^{18}O initially in the sample. The above expression is only approximate since there is initially oxygen with mass-17 (^{17}O) in the samples at the oxygen natural abundance level of 0.037 atomic%. The factor of 2 is necessary to describe the total concentration of oxygen diffused into the sample from an annealing atmosphere containing equal parts of ^{18}O and ^{16}O.

DISCUSSION

Here, it is our intent to evaluate bulk diffusion in the Yb_2O_3/YBCO bilayer. Raw SIMS data are messaged using equation (1) to give the concentration of diffused oxygen, Fig. 2, as a function of sputter time or depth in the bilayer. RBS results indicate thickness variations of about 10%, and the SIMS sputter time of these samples did vary also, indicating thickness variations. However, for the purposes of evaluating oxygen diffusion rates, all samples are assumed to have identical thicknesses. For graphical convenience, the sputter time or depth into the sample is normalized to the thickest sample.

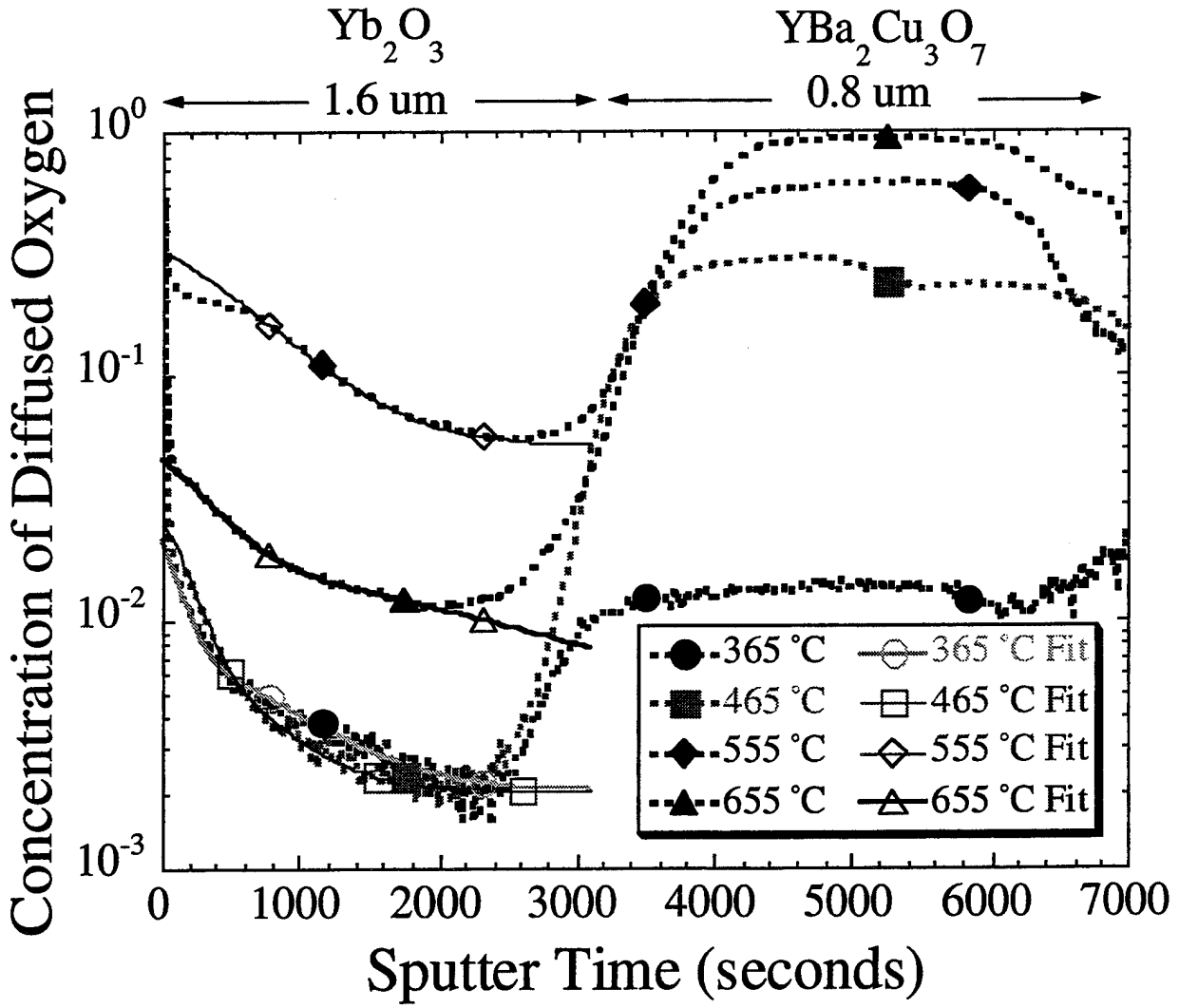

FIGURE 2. Converted SIMS data showing concentration of diffused oxygen as a function of depth into the Yb_2O_3/YBCO bilayer on (001) MgO substrate.

The diffusion behavior of oxygen in the Yb_2O_3 layer can be broken into two components, short circuit and bulk diffusion. These two types of diffusion can be independently modeled. Short circuit diffusion occurs due to pinholes, grain boundaries, particulate and other film imperfections, and depends on extrinsic factors like film deposition method and deposition parameters. Bulk diffusion is an intrinsic factor that is only dependent upon the material. It is the bulk diffusion rate that is of concern in HTSC multilayer structures, especially when the film has few imperfections.

In Fig. 2, oxygen diffusion in the Yb_2O_3 layer is modeled using a semi-infinite plane sheet solution [22] of the form:

$$C(x,t) = K_B(C_M - C_B)\sqrt{t}\left(1 - erf\left[\frac{x}{2\sqrt{D_B \cdot t}}\right]\right) + K_F(C_M - C_B)\sqrt{t}\left(1 - erf\left[\frac{x}{2\sqrt{D_F \cdot t}}\right]\right) + C_B \qquad (2)$$

where $C(x,t)$ is the concentration of diffused oxygen in the bilayer at depth x for annealing time t, K_B and K_F are a measure of the surface sorption associated with the bulk and fast diffusion component, C_M is the maximum concentration of diffused oxygen, C_B is the concentration (natural abundance level) of ^{18}O initially in the sample, *erf* is the error function, and D_B and D_F are the diffusivity in the bulk material and fast diffusion component, respectively.

The above solution fits the experimental conditions which are far from equilibrium for the dielectric layer. Note the dielectric layer is relatively thick compared to the depth to which bulk diffusion occurs in the dielectric. Also note that the concentration of diffused oxygen at the surface of the dielectric layer does not instantaneously rise to a final equilibrium value but rather increases toward an equilibrium value as a function of time. The terms $K(C_M - C_B)(t^{0.5})$ are used to model this behavior. The first and second terms in equation (2) arise due to bulk and short circuit diffusion, respectively. The final term, C_B, is due to the initial natural abundance level of ^{18}O in the sample.

Using the experimental conditions of C_M=1, C_B=0.00204 and the appropriate annealing time, Table 1, the experimental data are simulated, Fig. 2, by adjusting the parameters K_B, K_F, D_B and D_F. Table 1 lists values for K_B, K_F, D_B and D_F which give the reasonably good fits to the experimental data as shown in Fig. 2. Due to film surface roughness, SIMS depth resolution is estimated to be about 200 Å for this experiment. Film thickness variations are estimated to be 10% or ±1600 Å. The upper and lower limits of diffusivity, Table 1, are estimated (using only the first term in equation (2)) by adjusting D_B while using the simulated values for K_B, C_M, C_B and t until the 33% point of full surface concentration moves to ±1800 Å from its original simulated position. The bulk diffusivity with estimated upper and lower limits, Table 1, are used

in the Arrhenius plot, Fig. 3.

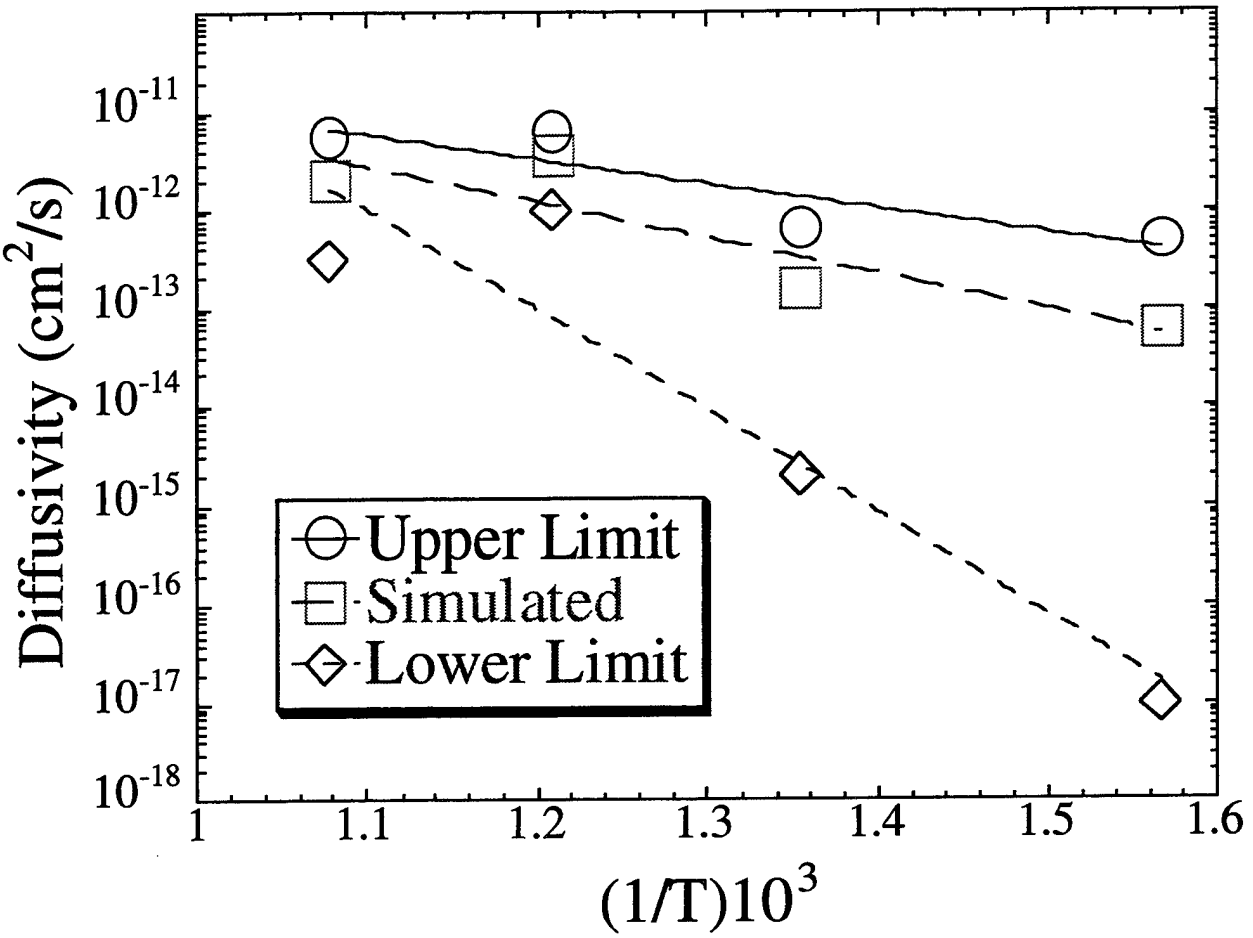

FIGURE 3. Simulated as well as estimated upper and lower limits for oxygen diffusivity in Yb_2O_3 are shown as symbols in the Arrehnius plot. The lines represent least squares fit to the data.

Using an equation of the form:

$$D = D_O \exp\left(\frac{-Q}{kT}\right) \tag{3}$$

where k is Boltzmann's constant, Q is the activation energy and T is the diffusion temperature, a least squares fit is obtained for each set of diffusivity values, and simulated as well as estimated upper and lower diffusion limits. The values for D_O, Q and the correlation or fitting factor, R, are reported in Table 2. The fit to the upper, lower and simulated diffusivity values yields the lowest, highest and most probable activation energies of 0.50, 0.73 and 2.03 eV, respectively. The lowest, highest and most probable values for D_O are 3.42×10^{-9}, 1.75×10^{-1} and 3.10×10^{-8} $cm^2\ s^{-1}$, respectively. By comparing these diffusivity values with those for polycrystalline YBCO [14] (which is the likely diffusion behavior of thin single crystal-like YBCO thin films), Yb_2O_3 will impede oxygen diffusion in underlying YBCO layers at temperatures greater than

about 500 °C.

Table 1. Fitting Parameters and Diffusion Values For Yb_2O_3.

T(°C)	Time (10^2 sec)	K (10^{-4})		D_F (10^{-9} cm^2s^{-1})	D_B (10^{-14} cm^2s^{-1})		
		K_B	K_F		Min.	Sim.	Max.
365	7.2	2.75	1.30	0.002	0.001	6	50
465	5.4	4.40	1.50	0.0015	0.2	16	65
555	3.0	88.0	18.0	3	100	360	650
655	1.5	12.50	7.90	0.09	30	200	550

The short circuit diffusion component which extends all the way to the YBCO layer allows a large uptake of ^{18}O into the YBCO layer. Note that there is always a larger concentration of ^{18}O in the YBCO film than in the fast diffusion component of the Yb_2O_3 layer. It can be argued that film edge effects, that is, diffusion of oxygen along the plane of the YBCO film, cannot account for the level of ^{18}O observed in the YBCO layers. Using the sample dimensions, it would take diffusivities on the order of 10^{-6} to 10^{-5} cm^2 s^{-1} to account for the maximum ^{18}O concentrations seen in the sample annealed at 450 °C. Therefore, short circuit diffusion paths through the Yb_2O_3 layer account for the large concentrations of ^{18}O observed in the YBCO layers. Portions of the YBCO film are in direct contact with the annealing atmosphere via pinholes through the dielectric. Oxygen is sorbed at the YBCO surface, diffuses along the *a* and *b* crystallographic axes and along defects in the *c* axis direction.

Table 2. Diffusion Coefficients For Yb_2O_3.

	D_o (10^{-8} cm^2s^{-1})	Q (eV)	R
Min.	0.342	0.50	0.771
Simulated	3.10	0.73	0.493
Max.	1.75×10^7	2.03	0.008

SUMMARY

While the diffusion rate of oxygen in thin single layer YBCO films has been of little concern due both to the rapid diffusion of oxygen along the *a* and *b* crystallographic axes and the defect nature of the material which provides short circuit diffusion paths along the slow diffusing *c* axis direction, diffusion of oxygen through buffer and dielectric layers in HTSC multilayer structures is of concern in multilayer device processing. It is important to determine the rate of oxygen diffusion through each material used in the multilayer structure so that proper annealing cycles can be used during device processing. We have investigated the rate of oxygen diffusion through Yb_2O_3. The diffusion rate of oxygen in this material is less than (5.0, 6.5, 65.0 and 55.0) x 10^{-13} $cm^2\ s^{-1}$ at 365, 465, 555 and 655 °C, respectively. For high quality pinhole free films of Yb_2O_3, oxygen uptake into an underlying YBCO layer will be impeded for temperatures greater than about 500 °C and ultimately longer annealing cycles will be required to fully oxygenate underlying YBCO layers in multilayer structures.

REFERENCES

1. J.G. Bednorz and K. A. Müller, "Possible High T_c Superconductivity in the Ba-La-Cu-O System," Z. Phys. B **64**, pp. 189-193 (1986).
2. N. Newman and W.G. Lyons, "Review: High-Temperature Superconducting Microwave Devices: Fundamental Issues in Materials, Physics, and Engineering," J. Supercond. **6**(3), pp 119-160 (1993).
3. E. Belohoubek, D. Kalokitis, A. Fathy, E. Denlinger, A. Piqué, X.D. Wu, S.M. Green and T. Venkatesan, "High Temperature Superconducting Components For Microwave Systems," Appl. Supercond. **1**(10-12), pp. 1555-1573 (1993).
4. Many excellent articles on HTSC devices appear in the Proceedings of the 1990 Applied Superconductivity Conference, IEEE Trans. Magn. **27**(2) Part IV(1991).
5. Many excellent articles on HTSC devices appear in the Proceedings of the 1992 Applied Superconductivity Conference, IEEE Trans. Appl. Supercond. **3**(1) Part IV(1993).
6. R. Simon, "High-T_c Thin Films and Electronic Devices," Physics Today **44**(6). pp. 64-70 (1991).
7. D.B. Chrisey and A. Inam, "Pulsed Laser Deposition of High T_c Superconduting Thin Films for Electronic Device Applications," MRS Bulletin **XVII**(2), pp. 37-43 (1992).
8. A. Oishi, H. Teshima, K. Ohata, H. Izumi, S. Kawamoto, T. Morishita, and S. Tanaka, "Y_2O_3 Single Crystalline Substrate For Epitaxial Growth of High T_c Superconducting Thin Films," Appl. Phys. Lett., **59**(15), pp. 1902-1904 (1991).
9. J. Hudner, M. Östling, H. Ohlsén, L. Stolt, P. Nordblad, M. Ottosson, J.C. Villegier, H.

Moriceau, F. Weiss and O. Thomas, "Preparation of $YBa_2Cu_3O_{7-\delta}/Y_2O_3$ Multilayers Using Coevaporation and Atomic Oxygen," J. Appl. Phys. **73**(6), pp. 3096-3098 (1993).

10. A. Catana and J-P. Locquet, "Domain Growth of Dy_2O_3 Buffer Layers on $SrTiO_3$," J. Mater. Res. **8**(6), pp. 1373-1378 (1993).
11. T. Wiktorczyk and C. Wesolowska, "Dielectric Properties of Ytterbium and Dysprosium Oxide Films Deposited By Electron Beam Evaporation," Vacuum **37**(1-2), pp. 107-109 (1987).
12. Y.S. Touloukian, R.K. Kirby, R.E. Taylor and T.Y.R. Lee, *Thermophysical Properties of Matter: Thermal Expansion Nonmetallic Solids*, Vol. 13, IFI/Plenum, pp. 435-437 (1977).
13. R.H. Hammond and R. Bormann, "Correlation Between the In Situ Growth Conditions of YBCO Thin Films and the Thermodynamic Stability Criteria," Physica C **162-164**, pp. 703-704 (1989).
14. Y. Ikuma and S. Akiyoshi, "Diffusion of Oxygen in $YBa_2Cu_3O_{7-y}$," J. Appl. Phys. **64**(8), pp. 3915-3917 (1988).
15. S.J. Rothman, J.L. Routbort, U. Welp and J.E. Baker, "Anisotropy of Oxygen Tracer Diffusion in Single-crystal $YBa_2Cu_3O_{7-\delta}$," Phys. Rev. B **44**(5), pp. 2326-2333 (1991).
16. S.I. Bredikhin, G.A. Emelchenko, V.S. Shechtman, A.A. Zhokhov, S. Carter, R.J. Chater, J.A. Kilner and B.C.H. Steele, "Anisotropy of Oxygen Self-Diffusion in $YBa_2Cu_3O_{7-\delta}$ Single-Crystals," Physica C **179**(4-6), pp. 286-290 (1991).
17. S. Tsukui, T. Yamamoto, M. Adachi, Y. Shono, K. Kawabata, N. Fukuoka, S. Nakanishi, A. Yanase and Y. Yoshioka, Direct Observation of O-18 Tracer Diffusion in a $YBa_2Cu_3O_y$ Single Crystal by Secondary Ion Mass Spectrometry," Jpn. J. Appl. Phys., **30**(6A), pp. L973-L976 (1991).
18. H.M. Smith and A.F. Turner, "Vacuum Deposited Thin Films Using a Ruby Laser," Appl. Opt. **4**(1), pp. 147-148 (1965).
19. D. Dijkkamp, T. Venkatesan, X.D. Wu, S.A. Shaheen, N. Jisrawi, Y.H. Min-Lee, W.L. McLean and M. Croft, "Preparation of Y-Ba-Cu Oxide Superconducting Thin Films Using Pulsed Laser Evaporation From High T_c Bulk Material," Appl. Phys. Lett. **51**(8), pp. 619-621 (1987).
20. J.D. Doss, D.W. Cooke, C.W. McCabe and M.A. Maez, "Noncontact Methods Used For Characterization of High-T_c Superconductors," Rev. Sci. Instrum. **59**(4), pp. 659-661 (1988).
21. S.C. Tidrow, W.D. Wilber, A. Tauber, S.N. Schauer, D.W. Eckart, R.D. Finnegan & R.L. Pfeffer, "Oxygen Diffusion Through Dielectrics: A Critical Parameter In HTSC Multilayer Technology," submitted to Journal of Materials Research.
22. J. Crank, *The Mathematics of Diffusion*, 2nd Edition, Oxford Univ. Press (1979).

ARMY RESEARCH LABORATORY
PHYSICAL SCIENCES DIRECTORATE
MANDATORY DISTRIBUTION LIST

Defense Technical Information Center*
ATTN: DTIC-OCC
8725 John J. Kingman Rd STE 0944
Fort Belvoir, VA 22060-6218
(*Note: Two DTIC copies will be sent from STINFO office, Ft. Monmouth, NJ)

Director
US Army Material Systems Analysis Actv
ATTN: DRXSY-MP
(1) Aberdeen Proving Ground, MD 21005

Commander, AMC
ATTN: AMCDE-SC
5001 Eisenhower Ave.
(1) Alexandria, VA 22333-0001

Director
Army Research Laboratory
ATTN: AMSRL-D (John W. Lyons)
2800 Powder Mill Road
(1) Adelphi, MD 20783-1197

Director
Army Research Laboratory
ATTN: AMSRL-DD (COL Thomas A. Dunn)
2800 Powder Mill Road
(1) Adelphi, MD 20783-1197

Director
Army Research Laboratory
2800 Powder Mill Road
Adelphi, MD 20783-1197
(1) AMSRL-OP-SD-TA (ARL Records Mgt)
(1) AMSRL-OP-SD-TL (ARL Tech Library)
(1) AMSRL-OP-SD-TP (ARL Tech Publ Br)

Directorate Executive
Army Research Laboratory
Physical Sciences Directorate
Fort Monmouth, NJ 07703-5601
(1) AMSRL-PS
(1) AMSRL-PS-T (M. Hayes)
(1) AMSRL-OP-FM-RM
(22) Originating Office

Advisory Group on Electron Devices
ATTN: Documents
Crystal Square 4
1745 Jefferson Davis Highway, Suite 500
(2) Arlington, VA 22202

Commander, CECOM
R&D Technical Library
Fort Monmouth, NJ 07703-5703
(1) AMSEL-IM-BM-I-L-R (Tech Library)
(3) AMSEL-IM-BM-I-L-R (STINFO Ofc)

Deputy for Science & Technology
Office, Asst Sec Army (R&D)
(1) Washington, DC 20310

HQDA (DAMA-ARZ-D/
Dr. F.D. Verderame)
(1) Washington, DC 20310

Director
Naval Research Laboratory
ATTN: Code 2627
(1) Washington, DC 20375-5000

USAF Rome Laboratory
Technical Library, FL2810
ATTN: Documents Library
Corridor W. STE 262, RL/SUL
26 Electronics Parkway, Bldg. 106
Griffiss Air Force Base
(1) NY 13441-4514

Dir. ARL Battlefield
Environment Directorate
ATTN: AMSRL-BE
White Sands Missile Range
(1) NM 88002-5501

Dir. ARL Sensors, Signatures,
Signal & Information Processing
Directorate (S31)
ATTN: AMSRL-SS
2800 Powder Mill Road
(1) Adelphi, MD 20783-1197

Dir. CECOM Night Vision/
Electronic Sensors Directorate
ATTN: AMSEL-RD-NV-D
(1) Fort Belvoir, VA 22060-5806

Dir. CECOM Intelligence and
Electronic Warfare Directorate
ATTN: AMSEL-RD-IEW-D
Vint Hill Farms Station
(1) Warrenton, VA 22186-5100

Cdr. Marine Corps Liaison Office
ATTN: AMSEL-LN-MC
(1) Fort Monmouth, NJ 07703-5033